

THEORETICAL AND EXPERIMENTAL INVESTIGATIONS OF MICRO ROBOTS BASED ON PIEZOELECTRIC TRIANGULAR PLATES

Vitalij Chigarev (a), Klaus Zimmermann (b), Felix Becker (c), Vladimir Minchenya (d)

(a) Ing., Belarusian National Technical University, Minsk, Belarus

(b) Univ.–Prof. Dr.–Ing. habil., Technische Universität Ilmenau, Germany

(c) Dr.–Ing., Technische Universität Ilmenau, Germany

(d) Dr.–Ing., Prof., Belarusian National Technical University, Minsk, Belarus

ABSTRACT

The creation of mobile miniature robots is an advanced and promising branch of modern engineering. The most important issues in the design of such robots are the development of propulsion and energy systems. The use of miniature electromechanical systems in the technological world is growing rapidly. Considering new applications the piezoelectric drive is a practical base to create miniature robots which move on different surfaces and in different media. Due to the small dimensions and low energy supply the development of piezoelectric platforms for miniature robots in the form of spheres, cylinders, plates with support rods can effectively solve many theoretical and practical problems.

To study complex stress-strain states of plate-platforms for miniature robots methods of numerical analysis (finite element calculation) are used. This allows to obtain solutions of boundary value problems for plates with various shapes in conditions of a controlled resonance. This results can be compared with experimental data. This approach leads to a significant reduction of the design costs.

Index Terms - piezoelectric platform, the resonance frequency, antiresonance, vibromotors of miniature robots, supporting rods, wave attractors, tripod, hexapod, ultrasonic actuator, piezoelasticity.

1. INTRODUCTION

Creating miniature mobile robot platforms in the form of plates, shallow shells, using vibrating systems as a drive are intensively discussed in recent years [1-6]. The sources of vibration (drive with an eccentric, piezoelectric drive) is directly mounted on the platform, equipped with limbs that come in contact with a supporting surface. Due to this contact translational and rotational movements of the miniature robot are possible. The transfer of vibrational energy from the actuator to the plate is associated with loss of energy in the plate material.

Therefore, the creation of miniature robots with a piezoelectric plate is energetically more efficient [7-10]. Also from the control point of view a piezoelectric platform is more effective. It provides a necessary control accuracy due to the choice of scheme electroded, shapes, designs, materials, weight. This gives the opportunity to design a wide range of miniature robots for various applications. One of the design tasks includes the definition of the desired resonance spectrum (own) and antiresonance frequency of which occurs the effective control of the state of miniature robot.

The platform model for a miniature robot installed on a piezoelectric plate secures autonomous motion in the presence of a battery, microprocessor, sensors and actuators on board. Conversion of electrical energy into mechanical energy occurs in the piezoelectric, and the transfer of mechanical energy is carried by elastic waves that create movement of elements of the plate and the associated limbs.

A miniature robot is a complex system so that the spectrum of eigenfrequencies of the structure as a whole is determined by the distributions of natural frequencies of components. The main eigenfrequencies belong to the plate-platform. So, the main part of the spectrum is determined by the geometry and the material of the piezoelectric plate.

2. MODELING DYNAMICS OF THE TRIPOD WITH VERTICAL ORIENTATION OF THE PLATFORM IN THE PLANE

Consider a rectangular piezoelectric plate, the middle plane of which coincides with a vertical coordinate plane XOZ , figure 2.1, and its geometric model, figure 2.2.

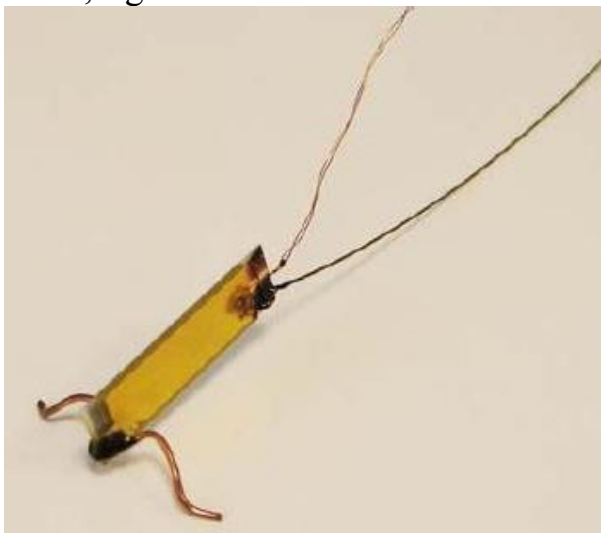


Figure 2.1. – Physical prototype of the platform on three support rods

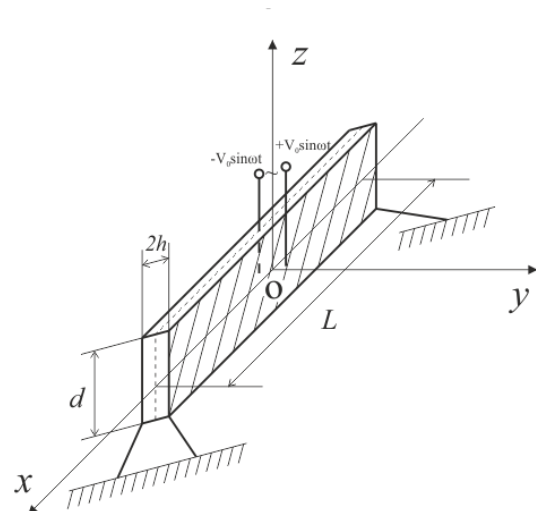


Figure 2.2. – Scheme of model platform with a vertical orientation on three support rods

The size of the plate fulfill the conditions $|x| < L$, $|y| < \frac{h}{2}$, $|z| < d$.

To the plate at points $x = L$, $y = \pm h$ and $x = -L$, $y = 0$ are rigidly attached three elastic rods of length l , by which the plate is in contact with the plane (unilateral constraints). The rods can slide or come off plane. The lateral planes $y = \pm h$ are electroded. When $t > 0$ they are affected by electric potentials $\varphi_0^\pm = \pm V_0 \sin \omega t$. The end of the plane $x = \pm L$, $|y| < h$ electroded, and they are affected by electric potentials.

Suppose that $h \leq d \ll L$, then the vibrations of the plate can be considered as transverse vibrations of a rod, i.e. the case of the Timoshenko beam [11-15] is considered.

Compared to the purely elastic variant in this case, the beam oscillates under the influence of electric fields. As know, the Timoshenko beam model takes into account the rotational inertia of the cross section and the shear deformation. Shear deformation distorts the flat cross section, which affects the dynamics section, which bonded the two supporting rod.

In the section $x = -L$ where the pinned single rod is in the median plane, this effect is absent. It was noticed [15] that with increasing frequency the influence of the transverse shear strains increases. This is due to the increase in the number of flexural waves per unit length of the rod.

Using piezoelectric elastic analogy, according to which the effective stiffness of piezoelectric materials is increasing [11-15], for the investigations the Timoshenko equation with arbitrary coefficients is considered. In general, the Timoshenko equation describing the free vibrations of the beam has the form

$$\frac{\partial^2 v}{\partial t^2} + a_1 \frac{\partial^4 v}{\partial x^4} - a_2 \frac{\partial^4 v}{\partial t^2 \partial x^2} + a_3 \frac{\partial^4 v}{\partial t^4} = 0. \quad (2.1)$$

Introducing new variables [16]

$$\eta = x, \quad \tau = t - \omega(x), \quad (2.2)$$

the transition to the derivative $\frac{\partial}{\partial \eta}$ in equation (2.1) denotes differentiation in the direction tangential to the line $t = \omega(x)$, $\frac{\partial}{\partial \tau}$ – in the direction of τ non-tangent to it. Lines $t = \omega(x)$ when $\tau = 0$ and $t = \omega(x) + \text{const}$ when $\tau = \text{const}$ are the characteristics (lines of discontinuity) field values.

In the new variables equation (2.1) has the form

$$\begin{aligned} & \frac{\partial^4 v}{\partial \tau^4} (a_1 \omega'^4 - a_2 \omega'^2 + a_3) + \frac{\partial^4 v}{\partial \tau^3 \partial \eta} (-a_1 4\omega'^3 + a_2 2\omega') + \\ & + \frac{\partial^4 v}{\partial \tau^2 \partial \eta^2} (a_1 6\omega'^2 - a_2) + \frac{\partial^4 v}{\partial \tau \partial \eta^3} (-a_1 4\omega') + \frac{\partial^4 v}{\partial \eta^4} a_1 + \frac{\partial^2 v}{\partial \tau^2} = 0. \end{aligned} \quad (2.3)$$

On the characteristics of the conditions that express the smoothness of all the lower derivatives are as follows:

$$\frac{\partial^2}{\partial \tau^2} \left(\frac{\partial^i v}{\partial \eta^i} \right) = 0; \quad \frac{\partial^4 v}{\partial \tau^4} \neq 0, \quad (i + s = 4, s < 4, i = 0, 1, 2, 3, 4). \quad (2.4)$$

From conditions (2.4) and equation (2.3) follows the equation for the characteristics:

$$a_1 \omega'^4 - a_2 \omega'^2 + a_3 = 0. \quad (2.5)$$

Two roots of the equation (2.5) have a physical meaning.

$$C_k = \sqrt{k} C_B, \quad C_B = \sqrt{E/\rho}, \quad (2.6)$$

where k – correction factor calculated by the formula

$$k = \frac{1}{J} \int_{S_1} f(y) y dy. \quad (2.7)$$

Here $f(y)$ is a function characterizing the shape of the distortion of the plane, which is chosen so that the distribution of shearing stresses in the section is the same as calculated by the formula of Zhuravsky [15]:

$$T_{xy} = \frac{QS}{Jb}. \quad (2.8)$$

Then we have

$$\frac{df}{dy} = -\frac{S_1 S(y)}{Jb}, \quad (2.9)$$

where S_1 – the cross-sectional area, J – moment of inertia. For a rectangular section $k = 1, 2$.

We have the ratio

$$\Psi = \frac{\partial v}{\partial x} - k\varphi, \quad (2.10)$$

where Ψ is the angular deformation of the bending, γ – angular shear strain, φ – describes the longitudinal offset.

$$u(x, y, z, t) = -\frac{\partial v}{\partial x} y + \varphi(x, t) f(y). \quad (2.11)$$

In (2.6) C_k is the velocity of propagation of shear waves, C_B – the propagation speed of bending waves, indicating that the Timoshenko equations to a hyperbolic type.

With decreasing the wavelength, a growing deplanation section [15,16] can be observed. That is essential for the considered model of the miniature robot in cross-section, where there are two limbs (rod).

Let us now consider the model of a core-plate from piezoelectric material to which an electric field is applied. Equation (2.1) describing the purely elastic

beam by Timoshenko, is supplemented by the equation for the electric potential (equations of electroelasticity) [11-15].

$$\begin{aligned} \frac{\partial^2 v_1}{\partial t^2} + \tilde{a}_1 \frac{\partial^4 v_1}{\partial x_1^4} - \tilde{a}_2 \frac{\partial^4 v_1}{\partial t_1^2 \partial x_1^2} + \tilde{a}_3 \frac{\partial^4 v_1}{\partial t_1^4} + \frac{\mu \eta \delta^3}{12} \left(\frac{\partial^4 \phi_1}{\partial x_1^4} - \frac{\partial^2 \phi_1}{\partial x_1^2 \partial t_1^2} \right) + \frac{\delta}{12} \frac{\partial^2 \phi_1}{\partial x_1^2} = \\ = x_1^3 \left(\frac{\mu \delta}{72} \frac{\partial^4}{\partial t_1^4} - \frac{1}{6 \delta} \frac{\partial^2}{\partial t_1^2} \right) V_* - x_1 \left(\frac{1}{6} \frac{\partial}{\partial t_1^2} - \frac{\mu \delta}{72} \frac{\partial^4}{\partial t_1^4} - \frac{(1+\mu) \delta}{12} \frac{\partial^2}{\partial t_1^2} \right) v_*; \end{aligned} \quad (2.12)$$

$$\begin{aligned} \delta k_{31}^2 \frac{\partial^2 \phi_1}{\partial x_1^2} + \delta (k_s^2 \beta_0 - k_{31}^2 \mu_0) \frac{\partial^2 \phi_1}{\partial t_1^2} + \frac{\beta_0}{12} (1 - k_s^2) \delta^2 \frac{\partial^2 \phi_1}{\partial x_1^2} - \phi_1 = \\ = x_1^3 (k_s^3 \beta_0 - k_{31}^2 \mu_0) \frac{1}{6} \frac{\partial^2 V_*}{\partial t_1^2} + x_1 \left[(1 + k_{31}^2) - (k_s^2 \beta_0 - k_{31}^2 \mu_0) \frac{1}{6} \frac{\partial^2}{\partial t_1^2} \right] v_*; \end{aligned} \quad (2.13)$$

Equations (2.12), (2.13) written in dimensionless form taking into account following transformations

$$\begin{aligned} x_1 = \frac{x}{L}, \quad t_1 = \frac{t}{a}, \quad a^2 = \rho \frac{L^2}{C_{11}^*}, \quad \delta = \frac{h}{L}, \quad v_1 = \frac{v}{L}, \quad \phi_1 = \frac{12 e_{31}}{C_{11} h^2} \phi, \\ \mu = \frac{6 C_{11}^*}{5 C_{44}^E}, \end{aligned} \quad (2.14)$$

$$\eta = \frac{e_{15}}{12 e_{31}^*}, \quad \beta_0 = \frac{\vartheta_{11}^*}{\vartheta_{33}^*}, \quad \mu_0 = \frac{5 \mu}{6}, \quad v_* = \frac{12 V_1 e_{31}^*}{C_{11}^* h} \sin \omega a t_1,$$

$$\tilde{a}_1 = \frac{\delta^2}{12}, \quad \tilde{a}_2 = (1 + \mu) \frac{\delta^2}{12}, \quad \tilde{a}_3 = \mu \frac{\delta^2}{12}.$$

Equations (2.12), (2.13) are solved with initial conditions of the form

$$v_1 = \frac{\partial v_1}{\partial t_1} = 0, \quad \delta \left(1 - \frac{k_s^2}{1 + k_{15}^2} \right) \frac{\partial^2 v_1}{\partial t_1^2} - \frac{e_{15} \vartheta_{33}^*}{e_{31}^* \vartheta_{11}^*} \phi_1 = 0 \quad \text{при} \quad t_1 = 0; \quad (2.15)$$

$$\delta \left(1 - \frac{k_s^2}{1 + k_{15}^2} \right) \frac{\partial^3 v_1}{\partial t_1^3} - \frac{e_{15} \vartheta_{33}^*}{e_{31}^* \vartheta_{11}^*} \frac{\partial \phi_1}{\partial t_1} = 0 \quad \text{при} \quad t_1 = 0 \quad (2.16)$$

The rod-plate is supported on a plane by three bars under its own weight, preventing the rupture of unilateral constraint relations and the emergence of the vertical component of the displacement vector directed upwards. The horizontal component of the displacement depends on friction forces. Thus, the body is motionless, although the electric potential in the quasi-static approximation is nonzero. The boundary conditions have the form

$$v_1 = \frac{\partial^2 v_1}{\partial x_1^2} + \frac{1}{\delta} \phi_1 - \mu \frac{\partial^2 v_1}{\partial t_1^2} + \delta \mu \eta \frac{\partial^2 \phi_1}{\partial x_1^2} = 0, \quad \text{for} \quad x_1 = \pm 1; \quad (2.17)$$

$$\phi_1 = \pm V_*, \quad \text{for} \quad x = \pm 1. \quad (2.18)$$

Formulated initial and boundary conditions in the form (2.15)–(2.18) allow to search for the solution of equations (2.12), (2.13) by the method of separation of variables according to v_1 , φ_1 , i.e.,

$$\begin{aligned} v_1(x_1, t_1) &= \sum_{n=1}^{\infty} v_{1n}(t_1) \sin(\pi n x_1); \\ \varphi_1(x_1, t_1) &= \sum_{n=1}^{\infty} \varphi_{1n}(t_1) \sin(\pi n x_1). \end{aligned} \quad (2.19)$$

The representation (2.19) satisfy the boundary conditions in the form (2.17), (2.18) and the equations (2.12), (2.13). For finding the time dependence $\varphi_{1n}(t)$, we obtain a disjoint system of ordinary differential equations of the form

$$\begin{aligned} b_{4n} \frac{d^4 \varphi_{1n}}{dt_1^n} + b_{2n} \frac{d^2 \varphi_{1n}}{dt_1^n} + b_{0n} \varphi_{1n} &= f_{1n}^*(t_1), \quad n=1, 2, \dots; \\ b_{4n} &= \mu + \frac{12\mu\eta\delta^2\lambda_n^2(k_s^2\beta_0 - k_{31}^2\mu_0)}{12 + \beta_0(1 - k_s^2)\delta^2\lambda_n^2}; \\ b_{2n} &= (1 + \mu)\lambda_n^2 + \frac{12\delta}{12 + \beta_0(1 - k_s^2)\delta^2\lambda_n^2} \times \\ &\times \left[(\mu\eta\delta\lambda_n^4 - \lambda_n^2\delta^{-1})(k_s^2\beta_0 - k_{31}^2\mu_0) - \mu\eta\delta k_{31}^2\lambda_n^4 \right]; \\ b_{0n} &= \lambda_n^4 - \frac{12\delta k_{31}^2\lambda_n^2(\mu\eta\delta\lambda_n^4 - \lambda_n^2\delta^{-1})}{12 + \beta_0(1 - k_s^2)\delta^2\lambda_n^2}, \quad \lambda_n = n\pi; \\ f_{1n}^* &= f_{1n} + \frac{12\mu\eta\delta\lambda_n^4 - \lambda_n^2\delta^{-1}}{12 + \beta_0(1 - k_s^2)\delta^2\lambda_n^2} \left(f_{2n} + \frac{d^2 f_{2n}}{dt_1^2} \right); \\ f_{1n} &= \int_{-1}^1 f_1(x_1, t_1) \sin(n\pi x_1) dx_1, \quad f_{2n} = \int_{-1}^1 f_2(x_1, t_1) \sin(n\pi x_1) dx_1, \end{aligned} \quad (2.20)$$

where $f_1(x_1, t_1), f_2(x_1, t_1)$ are the right members of equations (2.12), (2.13) respectively.

The solution of equation (2.20) subject to the initial conditions has the form

$$\varphi_{1n} = Jm \left[\sum_{k=1}^4 C_{nk} e^{\alpha_{nk} t_1} \right] + \frac{(-1)^n 24V_1 e_{31}^* \Omega_\lambda \sin(\omega a t_1)}{\lambda_n C_{11}^* h \left[b_{4n} (\omega a)^4 - b_{2n} (\omega a)^2 + b_{0n} \right]}, \quad (2.21)$$

where α_{nk} – purely imaginary roots of the characteristic equation.

$$b_{4n} \alpha^4 + b_{2n} \alpha^2 + b_{0n} = 0; \quad (2.22)$$

$$\Omega_\lambda = \left[\frac{\mu(\omega a)^4}{\delta \lambda_n^2} - \frac{(\omega a)^2}{\delta} \left(1 + \mu + \frac{12}{\lambda_n^2 \delta^2} \right) - \frac{12 \lambda_n^2 (1 - (\omega a)^2 (\mu \eta \delta \lambda_n^2 - \delta^{-1}))}{12 + \beta_0 (1 - k_s^2) \delta^2 \lambda_n^2} \right] \times$$

$$\times \left[(k_s^2 \beta_0 - k_{31}^2 \mu_0) \frac{(\omega a)^2}{\lambda_n^2} + 1 + k_{31}^2 \right].$$

Four constants C_{nk} included in the solution to (2.21) satisfy the four relations

$$\begin{aligned} \text{Im} \sum_{k=1}^4 C_{nk} &= 0, \quad \text{Im} \sum_{k=1}^4 C_{nk} \alpha_{kn}^2 = 0; \\ \text{Im} \sum_{k=1}^4 C_{nk} \alpha_{kn} &= a_{1n}, \\ \text{Im} \sum_{k=1}^4 C_{nk} \alpha_{kn} \left[\alpha_{kn}^2 \left(\delta \left(1 - \frac{k_s^2}{k_{1s}^2} \right) - a_{0n} \right) - a_{0n} \delta k_{31}^2 \right] &= a_{2n}, \end{aligned} \quad (2.23)$$

where the coefficients a_{0n} , a_{1n} , a_{2n} have the form

$$\begin{aligned} a_{0n} &= 12 e_{15} \vartheta_{33}^* \left[e_{31}^* \vartheta_{31}^* (12 + \beta_0 (1 - k_s^2) \delta^2 \lambda_n^2) \right]^{-1}; \\ a_{1n} &= \frac{(-1)^n}{\lambda_n} \frac{12 V_1 e_{31}^*}{C_{11}^* h} \left[\frac{\omega a}{\delta \lambda_n^2} - \frac{2 \Omega_\lambda \omega a}{b_{4n} (\omega a)^4 - b_{2n} (\omega a)^2 + b_{0n}} \right]; \\ a_{2n} &= \frac{(-1)^n}{\lambda_n} \frac{12 V_1 e_{31}^*}{C_{11}^* h} \left[\frac{2 \Omega_\lambda \omega a}{b_{4n} (\omega a)^4 - b_{2n} (\omega a)^2 + b_{0n}} \times \right. \\ &\quad \times \left((\omega a)^2 \left(\delta - \frac{\delta k_s^2}{1 + \delta_{15}^2} - a_{0n} \right) + a_{0n} \delta k_{31}^2 \right) - \frac{(\omega a)^3}{\lambda_n^2} \left(1 - \frac{k_s^2}{1 + k_{15}^2} \right)^{-2} + \\ &\quad \left. + 2 a_{0n} (k_s^2 \beta_0 - k_{31}^2 \mu_0) \frac{(\omega a)^2}{\lambda_n} + 2 a_{0n} (\omega a) (1 + k_{31}^2) \right]. \end{aligned}$$

The natural frequencies determined from the characteristic equation (2.22), form a spectrum of resonant frequencies at which the tripod can move.

We introduce the notation [11-15]

$$\begin{aligned} \Omega_n^2 &= \frac{(\omega a)^2}{N_n^2 \lambda_n^2 (1 + k_{31}^2)}, \quad N_n^2 = \frac{\delta^2 \lambda_n^2}{12}; \\ b_{02} &= \frac{\beta_0 (1 - k_s^2) - 12 \mu \eta k_{31}^2}{1 + k_{31}^2}, \quad b_{22} = 1 + \mu + \beta_0 + k_{31}^2 \mu_0 - 2 \beta_0 k_s^2; \\ b_{24} &= \beta_0 (1 - k_s^2) (1 + \mu) - 12 \mu \eta [k_{31}^2 (1 + \mu_0) - k_s^0 \beta_0]; \end{aligned} \quad (2.24)$$

$$b_{42} = \beta_0(1 - k_s^2) + 12\eta(k_s^2\beta_0 - k_{31}^2\mu_0).$$

For frequency Ω_n based equations (2.20), (2.21), (2.22), (2.23) it turns out the characteristic equation of the form

$$\begin{aligned}\Omega_n^4 + A_n\Omega_n^2 + B_n &= 0; \\ A_n &= -\frac{1 + N_n^2b_{22} + N_n^4b_{24}}{\mu(1 + k_{31}^2)(1 + N_n^2b_{42})N_n^4}; \\ B_n &= \frac{1 + N_n^2b_{02}}{\mu(1 + k_{31}^2)(1 + N_n^2b_{n2})N_n^4}.\end{aligned}\tag{2.25}$$

The roots of the equation (2.25) form a spectrum of eigenfrequencies, which in some cases are easier to explore. For example, in the approximation of the hypothesis of straight normals, believing $C_{nn}^E \rightarrow \infty$, we will receive

$$\Omega_n^2 = \frac{1 + \beta_0 N_n^2 (1 + k_{31}^2)^{-1}}{1 + \beta_0 N_n^2 (1 + N_n^2)}.\tag{2.26}$$

If, in addition, put $\beta_0 = 0$, we get

$$\Omega_n^2 = 1.\tag{2.27}$$

Approximation following Rayleigh, Bernoulli–Euler assess the influence of transverse shear depending on the relative thickness of the plate. For thick plates, the transverse shifts exist already in the lowest frequencies. For relatively thin plates it is necessary to consider higher frequencies. For the described model of the miniature robot and for its design the spectrum of natural frequencies is important. For thicker plates, the robot begins to move already at lower frequencies, while the thin robot is correct for the beginning of the movement of excitation at higher frequencies. Deplanation cross section in the mounting of the two limbs, as shown by the experiments already at low frequencies provides a walking mode, moving miniature robot.

3. THE APPROXIMATE ANALYSIS OF THE TRIPOD AND HEXAPOD MODEL BASED ON A TRIANGULAR PLATE OF PIEZOELECTRIC MATERIAL

The problem of finding the natural modes and frequencies of vibration is determined by the shape vibrating system. For rectangular and circular plates the eigenforms can be found in an analytical closed form. For plates with an other geometry the definition of eigenforms is more difficult [16].

Consider the approach to some approximate solutions that can be used in the design of the tripod and hexapod based on triangular plates.

In the case of non-rectangular plates, in particular triangular, we introduce an oblique coordinate system

$$\xi_1 = x_1 - x_2 \tan \alpha, \quad \xi_2 = x_2 \sec \alpha, \quad (3.1)$$

and the system of linear equations of electroelasticity for displacements u_i and potential φ will take the form

$$C_{ijkl}^E \frac{\partial^2 u_k}{\partial x_i \partial x_j} + e_{kij} \frac{\partial^2 \varphi}{\partial x_k \partial x_j} = \rho \frac{\partial^2 u_i}{\partial t^2}; \quad (3.2)$$

$$e_{ikl} \frac{\partial^2 u_k}{\partial x_l \partial x_i} - \varepsilon_{ik} \frac{\partial^2 \varphi}{\partial x_k \partial x_i} = 0, \quad (3.3)$$

describing the oscillations of the plate, move on to variables ξ_1, ξ_2 . Transverse vibrations of a plate described by the function $W(\xi_1, \xi_2, t)$ we find with the method of separation of variables according to which the approximate representation of the mode shapes in the first approximation is obtained [15]

$$W_{mn} = f_{mn} F_m^{(1)}(\xi_1) F_n^{(2)}(\xi_2), \quad (3.4)$$

where $F_m^{(i)}$ the beam functions for the relevant boundary conditions.

According to the formula of Rayleigh–Ritz the approximate expression for the frequency has the form

$$\omega_{mn} = \pi^2 \sec \alpha \left(\frac{D}{\rho h} \right)^{1/2} \left\{ \frac{A_m^{(1)4}}{a_1^4} + \frac{A_n^{(1)4}}{a_2^4} + \frac{2}{a_1^2 a_2^2} \left[\nu B_m^{(1)} B_n^{(2)} + (1 - \nu) C_m^{(1)} C_n^{(2)} + \right. \right. \quad (3.5)$$

$$\left. \left. + 2 \sin^2 \alpha C_m^{(1)} C_n^{(2)} - 2 \sin \alpha \left(D_m^{(1)} E_n^{(2)} + D_n^{(E)} E_m^{(1)} \right) \right] \right\}^{1/2}.$$

The expression (3.4), (3.5) takes place for a purely elastic plate. The generalization to a piezoelectroelastic plate get through the application of the piezoelastic analogy, according to which piezoelastic material is described by the same ratios as a purely elastic problem with effective piezoelastic modules. Thus, the natural frequency for a piezoelastic plate can be obtained from (3.5), replacing the elastic moduli on piezoelastic. The coefficients A_m, B_m, C_m at various numbers of nodes of beam functions, and various combinations of terms on opposite sides of a rectangular plate [15]

$$\omega_m = \pi^2 \left(\frac{D}{\rho h} \left\{ \frac{A_m^2}{a_1^4} + \frac{A_n^2}{a_2^4} + \frac{2}{a_1^2 a_2^2} \left[\nu B_m B_n + (1 - \nu) C_m C_n \right] \right\} \right)^{1/2}. \quad (3.6)$$

The values of D_m and E_m depend on a combination of different boundary conditions.

Method oblique coordinate quite effective for plates of triangular shapes when the frequency is calculated by the method of Ritz, figure 3.1.

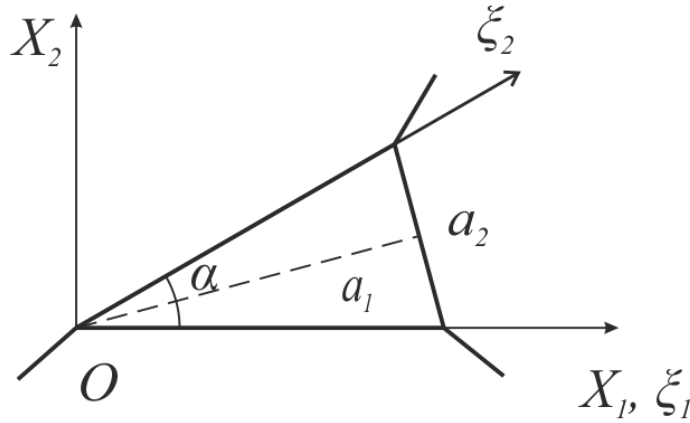


Figure 3.1. – Schematic representation of the model of the tripod (top view)

W has the form

$$W = \sum_m C_m f_m(\xi_1, \xi_2), \quad \text{ctg} \alpha = \frac{a_1}{a_2}, \quad \omega_* = \omega a_1^2 \left(\frac{\rho h}{D} \right)^{1/2}. \quad (3.7)$$

The coefficients C_n are according to the method of Ritz from the system of equations resulting from minimizing the expression

$$\begin{aligned} & \frac{\partial}{\partial C_n} \iint_S \xi_1 \left(\frac{\partial^2 W}{\partial \xi_1^2} \right)^2 - 4 \xi_2 \frac{\partial^2 W}{\partial \xi_1^2} \cdot \frac{\partial^2 W}{\partial \xi_1 \partial \xi_2} + \frac{2}{\xi_1} \left[(2 \xi_2^2 + \alpha^2 (1 - \nu)) \left(\frac{\partial^2 W}{\partial \xi_1 \partial \xi_2} \right)^2 \right. \\ & + (\xi_2^2 + \nu \xi_1^2) \frac{\partial^2 W}{\partial \xi_1^2} \cdot \frac{\partial^2 W}{\partial \xi_2^2} + 2 \xi_2 \frac{\partial W}{\partial \xi_2} \cdot \frac{\partial W}{\partial \xi_1} \left. \right] - \frac{4}{\xi_1^2} \left[\left(2 \xi_1^2 + \alpha^2 (1 - \nu) \right) \frac{\partial^2 W}{\partial \xi_1 \partial \xi_2} \cdot \frac{\partial W}{\partial \xi_1} + \right. \\ & + (\xi_2^2 + \xi_1^2) \frac{\partial^2 W}{\partial \xi_1 \partial \xi_2} \cdot \frac{\partial^2 W}{\partial \xi_2^2} \left. \right] + \frac{1}{\xi_1^2} \left[2 \left(2 \xi_2^2 + \alpha^2 (1 - \nu) \right) \left(\frac{\partial W}{\partial \xi_2} \right)^2 + \right. \\ & + 4 (\xi_2^2 + \alpha \xi_2^2) \frac{\partial W}{\partial \xi_2} \cdot \frac{\partial^2 W}{\partial \xi_2^2} + (\xi_2^2 + \alpha^2) \left(\frac{\partial^2 W}{\partial \xi_2^2} \right)^2 \left. \right] - \omega_*^2 \xi_1 W^2 \} d\xi_1 d\xi_2 = 0. \end{aligned} \quad (3.8)$$

The system of equations for finding C_n has a nonzero solution when the determinant is equal to zero. Functions $f_m(\xi_1, \xi_2)$ are taken from the beam approximations. Thus, an approximate solution of the problem is reduced to finding the coefficients C_n by minimizing (3.8). The equation describing radial oscillations for the axisymmetric problems in cylindrical coordinates, has the form

$$\frac{d^2 u_r}{dr^2} + \frac{1}{r} \frac{du_r}{dr} + \left(k^2 - \frac{1}{r^2} \right) u_r = 0, \quad k^2 = \rho \omega^2 / C_{11}^*. \quad (3.9)$$

The electric potential $\varphi(r, z)$ satisfies the equation

$$\frac{\partial^2 \varphi}{\partial r^2} + \frac{1}{r} \frac{\partial \varphi}{\partial r} + v^2 \frac{\partial^2 \varphi}{\partial z^2} = -z\mu \frac{1}{r} \frac{d}{dr} \left[r \left(\frac{d^2 u_r}{dr^2} + \frac{1}{r} \frac{du_r}{dr} - \frac{u_r}{r^2} \right) \right];$$

$$v^2 = \frac{\mathfrak{A}_{33}^*}{\mathfrak{A}_{11}^*}, \quad \mu = \frac{e_{15}^E C_{13}^E}{C_{33}^E \mathfrak{A}_{11}^*}.$$
(3.10)

On the lateral surface

$$\langle T_{rr} \rangle = 0, \quad D_r = 0 \quad \text{при} \quad r = a.$$
(3.11)

The solution (3.9) has the form

$$u_r(r) = \frac{2V_0 a e_{31}^*}{h} \frac{J_1(kr)}{\Delta(ka)}, \quad \Delta(ka) = C_{11}^* ka J_0(ka) - (C_{11}^E - C_{12}^E) J_1(ka),$$

$$k^2 = \frac{\rho \omega}{C_{11}^*},$$
(3.12)

where $J_0(x)$, $J_1(x)$ are Bessel functions. Equation (3.10) is solved by the method of separation of variables and expressions φ , E_r are solutions of ordinary differential equations. Figure 3.2 shows the dependence of coefficient of electromechanical communication $K(ka)$.

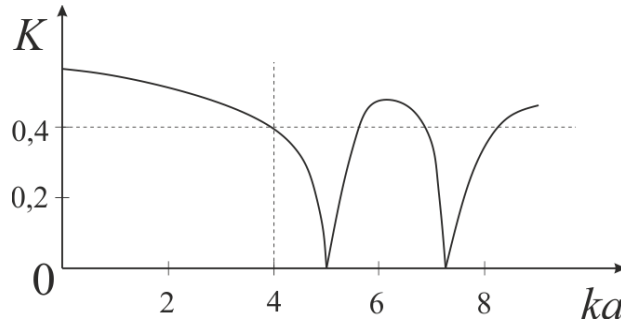


Figure 3.2. – The dependence of the electromechanical coefficient when the ratio between radius and wavelength $\lambda = k^{-1}$

From figure 3.2 it is seen that there are frequencies and radii of the plates, for which it is impossible to excite vibrations at these frequencies. In order to change the situation we change the topography of the electrodes. For example, we can make the system cut annular zones of the electrodes on the surfaces of the plate, use composites of the given structure [13].

The dynamics of the robot can be increased by changing the stiffness of the supporting limbs. It is possible to change the thickness of the vertices of the triangle variable, then due to the decrease of structural stiffness of the limbs the movement of the contact point increases significantly due to the effect of focus energy at the vertices of the tripod.

4. NUMERICAL CALCULATION OF STRUCTURAL ELEMENTS of MINIATURE ROBOTS WITH AN ULTRASONIC ACTUATOR

The computer simulation performed with the software ANSYS and SolidWorks shows the behavior of the microrobot under specified physical conditions. We can also analyze the impact of design changes to the basic model concerning its functionality for various applications. That allows us to choose the best modes of operation of the miniature system.

The study of free vibrations with a finite element model has allowed to obtain the stress-strain state of the system at any time and the eigenfrequencies of the system.

Figure 4.1 presents a finite element model of the basic microrobot with a round piezoelectric element and three executive elements of various configurations. By modeling the different working conditions of the system criteria for the best performance of the microrobot are obtained.

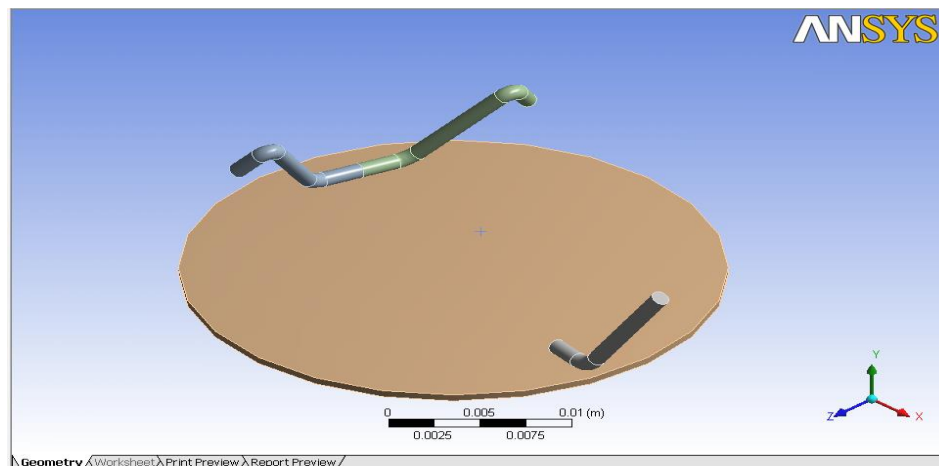
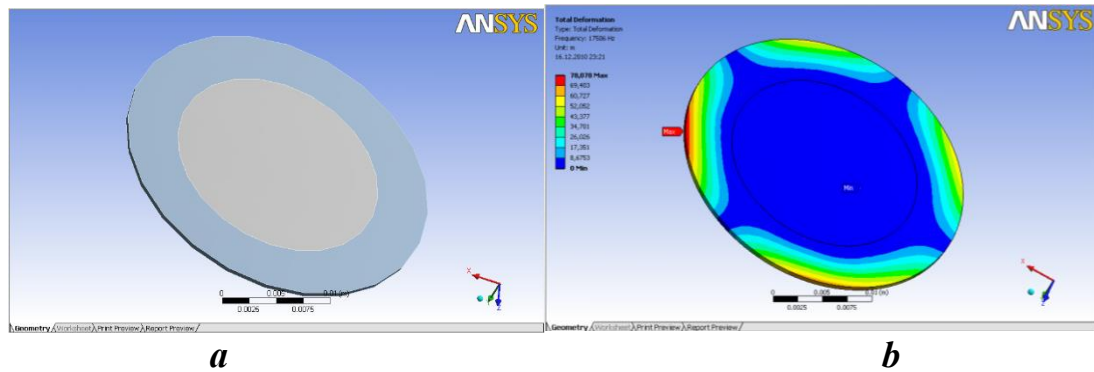


Figure 4.1. – The assembly of the microrobot with a round piezoelectric element in the software package "ANSYS Workbench"

First, a round piezoelectric element outside the assembly (figure 4.2) is modelled, which allowed to determine the shape of celebi at the specified frequency, and the maximum longitudinal and transverse vibrations of the plate.

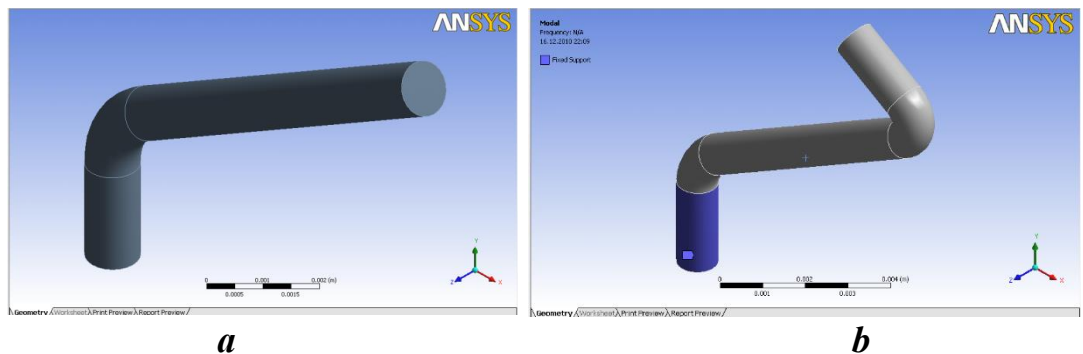


***a* – the piezoelectric element with a round shape and with a coating of piezoelectric ceramics;
b – the color scheme of the stress-strain condition of the plate
 Figure 4.2. – Piezoelectric element in ANSYS**

Figure 4.2 b presents the stress-strain state of the plate when the resonant oscillations for the five mode (frequency – 17506 Hz, amplitude 78,078 μm).

Analysis of the graphical data clearly shows the distribution of mode shapes in terms of parts. This allows only on the basis of empirical data to define frequencies in which the item can be used as a working body of the oscillating system.

For example, a three-tier control element figure 4.3 from the base assembly illustrates the convenience of this method for the study of systems operating at the resonance conditions.



***a* – two-tier, *b* – three-tier
 Figure 4.3. – The executive elements of the microrobot in ANSYS**

The efficiency of the moving system can be influenced the selection of the used eigenforms and the analysis of the stress-strain state.

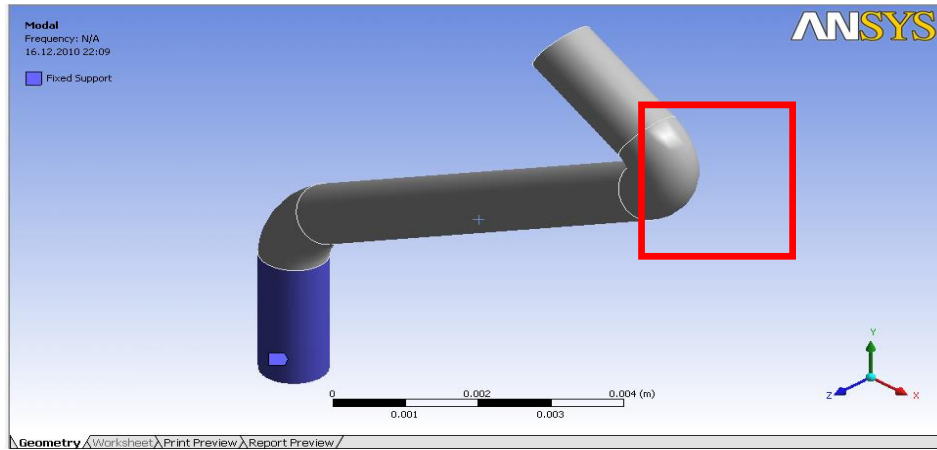
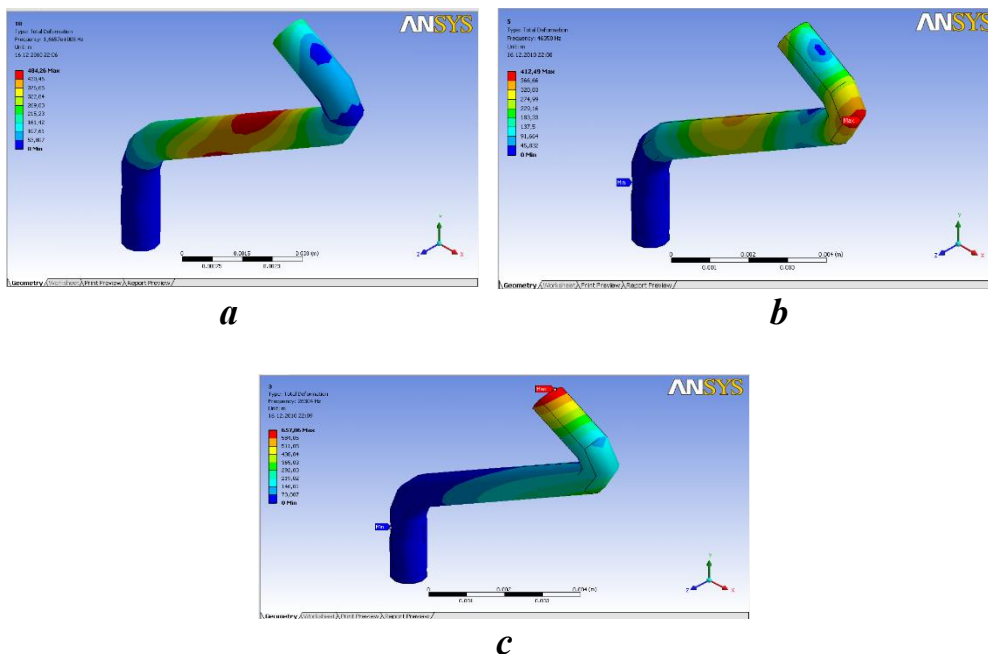


Figure 4.4. – Workspace design model three-tier actuator of the microrobot

Figure 4.4 shows the greatest deviation from the initial state under the influence of resonance. That vibrations lead to a maximum robot displacement.

In figure 4.5 a scheme of the stress distribution and deformations arising in elements of three-tier miniature robot over the entire volume details is shown. In figure 4.5 *a* – oscillation frequency $1,6657 \times 10^5$ Hz, and the amplitude $484,26 \mu\text{m}$; 4.5 *b* – frequency oscillations 46358 Hz, and the amplitude $412,49 \mu\text{m}$; 4.5 *c* – the oscillation frequency of the 26304 Hz, and the amplitude $657,06 \mu\text{m}$.



a for mode number 10; *b* – for mode number 5; *c* – for mode number 3

Figure 4.5. – Various eigenforms of the actuator

For mode number 10, see figure 4.5 *a* the working surface of the control element is not subjected to substantial deviation from the original state, therefore, the frequency cannot be "working". For mode number 5, see figure 4.5 *b*, involved in the working surface of the actuating element, the state diagram is marked with a sticker "Max" is ideal for design purposes. The point on the working surface, marked with sticker "Max", can be considered as a point of contact of the actuator to the surface. Mode number 3, see figure 4.5 *c* involved the tip part, which is also undesirable.

By the selection of suitable frequencies optimal modes of operation for the microrobot can be defined (efficient modes of operation).

To study the possibilities of actuators in the context of controlled resonance different types of actuators and their assemblies together with the piezoelectric elements were modeled and designed, figures 4.6 – 4.8.

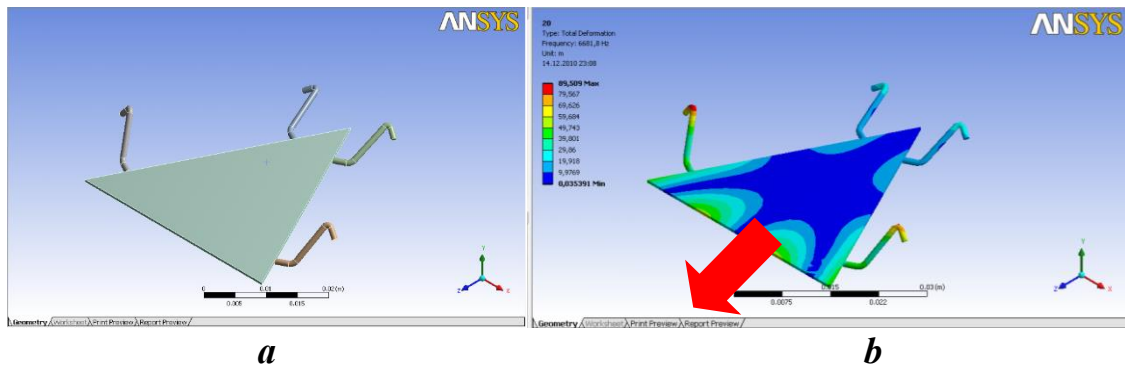


Figure 4.6. – The model (a) and the modes (b) of a miniature robot in form of a tripod

Figure 4.6 *b* presents the stress distribution and deformation during oscillations of the system with mode number 20 for 6683,8 Hz and an amplitude of 89,509 μm . The direction of motion in resonance shows the red arrow.

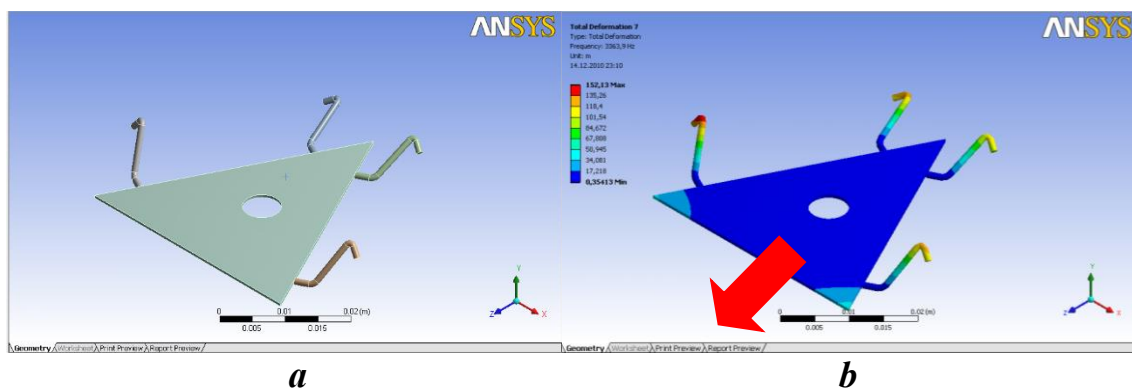


Figure 4.7. – The model of a triangle miniature robot with hole (a) and its eigenmodes (b)

Figure 4.7 *b* presents the stresses and deformations of the system with the mode number 12 for the oscillation frequency 3363,9 Hz and amplitude 152,13 μm . Figure 4.8 *b* shows the stress distribution and deformation during oscillations with mode number 15 for 3457,4 Hz and an amplitude of 138,85 μm .

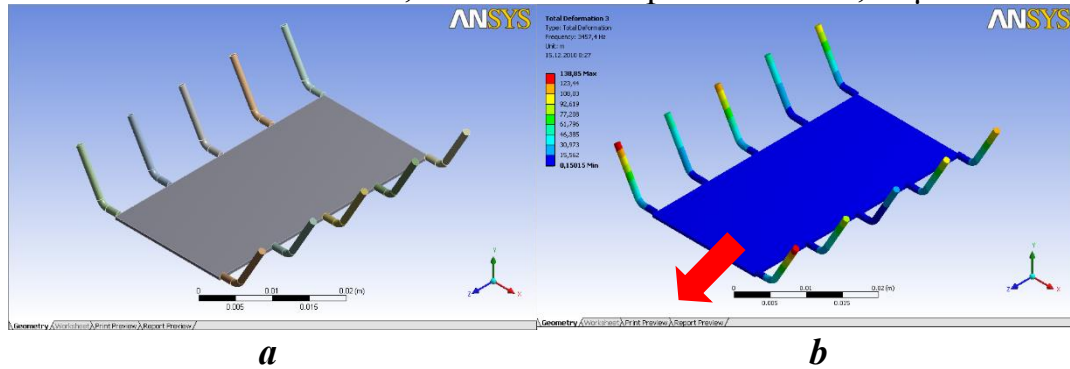


Figure 4.8. – The rectangular model of a miniature robot (a) and eigenmodes of the miniature robot (b)

The optimal ratio between the resonant frequencies of longitudinal and flexural vibrations of the piezodrive is achieved by matching the length of the control element and their bends in the spatial coordinate system.

The experimental study of the trajectory of the contact surface of the actuating element showed that by changing harmonic components of the longitudinal and flexural vibrations of piezoplates different trajectory of contact points of the executive elements are possible.

Figure 4.9 shows the basic scheme of the trajectories of contact points of the executive elements at different ratios of the amplitudes of the longitudinal and flexural vibrations of piezoceramic plates.

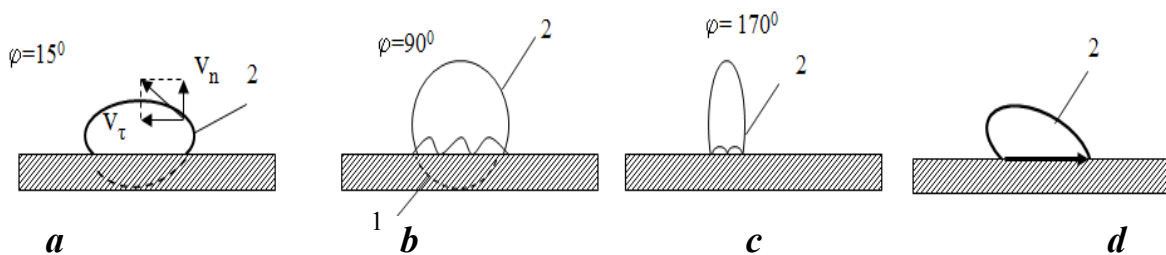


Figure 4.9. – The basic scheme of trajectories of the contact points of the executive elements of the microrobot with piezodrive

On figure 4.9 V_n – normal component of the velocity vector of the movement of the contact point, V_τ – tangential component of the velocity vector of the movement of the contact point, 1 – contact surface, 2 – the trajectory of the contact point.

Higher values appear normal component of the rebound of the contact point from the surface, see figure 4.9 *b, c*. Such vibro-impact mechanism leads to

unstable motion of the microrobot on a hard surface and to steady mode when driving on a rough surface. When driving on smooth surfaces, most preferred are small angles of contact, see figure 4.9 *a*. The trajectory of the contact point in case of unequal amplitudes of the longitudinal and bending vibrations are shown in figure 4.9 *d*. These cases correspond to zero tangential velocity component at the exit and at the entrance to the contact zone of actuator miniature robot, and its movement slows down.

5. CONCLUSION

In the design process of piezoelectric actuators for miniature robots, the problem on excitation in resonance mode of longitudinal vibration in plates and beams was solved. The robot made by a piezoelectric material can move along the plane with the help of actuators-rods, traversing-type “paddle”. Also solved was the problem of finding the natural modes and resonance frequencies for plates of non-rectangular and non-circular shapes. In particular, for the triangular plate, the method of transition to oblique coordinates was used. For regular polygons (hexagon) a method for finding the approximate natural modes and frequencies of vibration was developed.

The usage of FEM software leads to an efficient analysis of the functionality of systems in the context of controlled resonance and to the identification of best performance parameters.

REFERENCES

- [1] K. Zimmermann, I. Zeidis, C. Behn, Mechanics of terrestrial locomotion: with a focus on non-pedal motion systems, Springer-Verlag Berlin and Heidelberg GmbH & Co. KG, Berlin Germany, 309 p., 2010.
- [2] G. Maugin, Continuum mechanics of electromagnetic solids, Paris, France, 1988, (Mechanics of electromagnetic continua), translation from English: Vladimir Kiryushin ; under the editorship of I. M. Dunaev, V. Z. Parton, Moscow : Mir, 560 p., 1991.
- [3] E. Dieulesain, D. Royer, Ondes Elastiques Dans Les Solides, Masso et Co, (Elastic waves in solids: applications to signal processing), translation from FR. under the editorship of V. V. Lemanov, Moscow : Nauka, 424 p., 1982.
- [4] R. J. Bansevicius [etc.], “Some aspects of high frequency vibration displacements”, Nauch. Tr. universities Lit. SSR, Kaunas. Polytechnic. in-t. – Kaunas, vol. 3, No. 20, Pp. 317-323, 1973.
- [5] A. B. Smirnov, Mechatronics and robotics. System micrometric movements with piezoelectric actuators : proc. Handbook, St. Petersburg. : Izd-vo S.-peterb. state Polytechnic College. University, 160 p., 2003.

- [6] V. A. Dyachenko, A. B. Smirnov, “Piezoelectric device mechatronics”, mechatronics: mechanics, automatics, electronics, Informatics. No. 2, Pp. 38-46, 2002.
- [7] A. B. Smirnov, “Methods of calculation of elastic systems with bimorph piezoelectric transducers”, Izv. universities. Ser. Instrumentation, Vol. 46, No. 1, Pp. 48-54, 2003.
- [8] V. T. Minchenya [et al.], “The dynamics of the microrobot with three fulcrum on the planar surface”, 50. Internationales Wissenschaftliches kolloquium. Mechanical engineering from macro to nano, Techn. Hochsch. Ilmenau. – Ilmenau, 2005, P. 403–404, 19–23 September 2005.
- [9] B. Mazzelai [et al.], “A miniaturized mechatronics system inspired by plant roots for soil exploration”, IEEE/ASME Trans. on Mechatronics, Vol. 16, № 2. – P. 201–212, 2011.
- [10] F. Becker, V. Lysenko, V.T. Minchenya, O. Kunzo, K. Zimmermann, “Locomotion principles for microrobots based on vibrations”, Microactuators and Micromechanisms, Zentner L., Corves B., Brian J., Edwin Christian L. Proceeding of MAMM-2016, Ilmenau, Germany, , Springer-Verlag GmbH, Mechanisms and Machine Science 45, October 5-7, 2016.
- [11] V. Minchenia, V. Chigarev, K. Zimmerman, K. Abazza, “The dynamical of a microrobot with three fulcrums on the plane surface”, 50. Int. Wissenschaft. Kolloquium, p. 101-102, 19-23.09.2005
- [12] R. J. Bansevicius, K. M. Ragulskis, “A new form control element drive systems in vibromotors”, Nauch. Tr. universities Lit. SSR, Kaunas. Polytechnic. in-t. – Kaunas, vol. 3, No. 16, Pp. 296-307, 1972.
- [13] A. A. Pankov, “Statistical mechanics of composites”, Perm : Publishing house Perm. gos. tehn. University press, 479 p., 2009.
- [14] V. V. Lavrinenko, I. A. Kartashev, V. S. Wisniewski, Piezoelectric motors, Moscow : Energiya, 110 p., 1980.
- [15] V. Z. Parton, B. A. Kudryavtsev, Electromagnetoelastic piezoelectric and electric bodies, Moscow : Nauka, 470 p., 1988.
- [16] S. P. Timoshenko, S. Voinovich-Kreeper, Plates and shells, translation from English. V. I. Contout ; edited by G. S. Shapiro. – 2nd ed. revised. – M. : Science, 635 p., 1966.
- [17] E. Hogue, K. Choi, V. Komkov, Sensitivity Analysis for the design of structures, translation from English: S. Y. Ivanova, A. D. Larichev ; ed. V. Banichuk, M. : Mir, p. 428, 1988.

CONTACTS

Ing. V. Chigarev chigarev.vitalik@yandex.ru

Univ.–Prof. Dr.–Ing. habil. K. Zimmermann klaus.zimmermann@tu-ilmenau.de

Dr.–Ing. F. Becker felix.becker@tu-ilmenau.de

Dr.–Ing., Prof. V. Minchenya vladimir.minchenya@mail.ru